Controlled Growth of Gold Nanoparticles during Ligand Exchange

Leif O. Brown and James E. Hutchison*

Department of Chemistry and the Materials Science Institute University of Oregon, Eugene, Oregon 97403-1253

Received October 5, 1998

Metal nanocrystals have become a subject of intense interest in materials and physical chemistry. Their unique physical properties give rise to a wide variety of potential applications such as sensors, biochemical tagging reagents, optical switches, nanoelectronic devices, and catalysts.[1] Recently we reported the preparation of robust thiolate-stabilized gold nanoparticles by application of ligand exchange chemistry to the known species, $Au_{55}(PPh_3)_{12}Cl_6$.[2] A potential limitation of the ligand exchange approach is the inability to control the metal core size.

Here we demonstrate that the use of a primary amine ligand[3] such as 1-pentadecylamine (PDA)[4] in an exchange reaction leads to a nanocrystalline product with a highly reproducible, yet expanded core size. Growth of the core from 1.4 to 5 nm occurs in a controlled manner as observed by TEM and visible spectroscopy. Thus it is now possible to use ligand exchange methods to alter the physical size of the nanoparticle, as well as the ligand shell.

The ligand exchange chemistry between triphenylphosphine-stabilized gold nanoparticles (Au-TPP)[5] and PDA was investigated under a variety of conditions (see Table 1). Briefly,[6] Au-TPP is dissolved in CH_2Cl_2 (or $CHCl_3$) and stirred in the presence of excess PDA at room temperature, typically for ∼4 days. A golden precipitate of large insoluble nanocrystals may be observed when using CH_2Cl_2 as the solvent. This is usually excluded from the product mixture by filtration.[7] The remaining smaller nanocrystals are precipitated at reduced temperature and collected by filtration. Rinsing removes impurities to give the amine-stabilized nanocrystals (Au-PDA) as a golden film, soluble in CH_2Cl_2 or $CHCl_3$. Further conversion from amine-passivation to thiolate-passivation is possible.[8]

The product nanocrystals form deep red solutions exhibiting significant plasmon resonance ($\lambda_{max} = 525$ nm, see Figure 3 for a spectrum of a ∼5 nm diameter nanocrystal). In the solid state, thin films appear blue with a metallic reflectivity similar to that of plated gold ($\lambda_{max} \sim 590$ nm). Further characterization of the material was performed with use of TEM, XPS, and NMR.

A representative TEM (Philips CM-12, 120 kV accelerating voltage) of Au-PDA (prepared with use of a 1:4 mass ratio of Au-TPP to PDA) is given in Figure 1. A striking feature is the extended hexagonal ordering of the nanocrystals (some of which are clearly faceted), hinting at unusually narrow size dispersity. The size range for this sample is found to be 5.1 ± 0.8 nm, compared with 1.4 ± 0.4 nm for the Au-TPP starting material.[9] In addition, several pieces of evidence demonstrate the crystallinity of the sample: (i) interference fringes between lattice planes of different nanocrystals, (ii) diffraction from different nanocrystal orientations giving rise to both light and dark nanocrystals, and (iii) electron diffraction patterns corresponding to fcc packing. Further, the [111] lattice planes can be imaged by using tilted illumination (Figure 2). At a typical diameter of ∼20 lattice planes, the nanocrystals would comprise ∼4200 atoms to a first approximation.[10]

XPS is used to obtain information concerning the chemical composition of the nanocrystals. As expected, a single Au 4f

Table 1. Example Size Distribution Data (from TEM data) for Au-PDA Formed under Different Conditions

solvent[a]	ratio[b]	fraction[c]	mean ± std dev (nm)[d]
CH_2Cl_2	1:4	soluble	5.1 ± 0.8 [*5078*]
CH_2Cl_2	1:2	soluble insoluble	5.5 ± 0.9 [*772*] 7.2 ± 1.2 [*202*]
CH_2Cl_2[e]	1:0.1	soluble	5.2 ± 1.4 [*3426*]
$CHCl_3$[e]	1:2	soluble	4.1 ± 1.2 [*1978*]

[a] Reaction solvent. [b] Mass ratio of Au-TPP:PDA used. [c] Fraction used for analysis based on its solubility in the reaction solvent. [d] Core diameter. Value in brackets indicates the number of particles measured. [e] No permanent precipitate formed in these reactions.

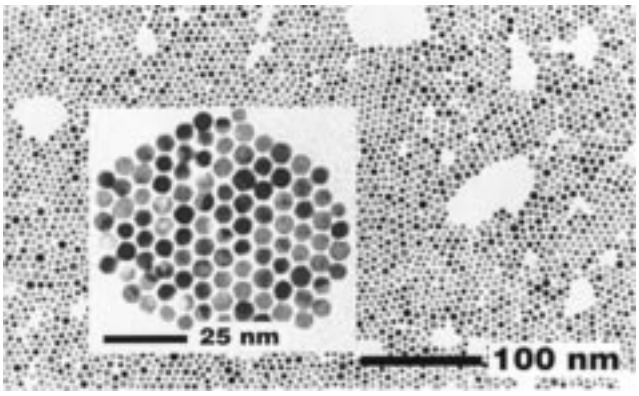

Figure 1. TEM of Au-PDA prepared with use of a 1:4 mass ratio of Au-TPP to PDA. Inset shows close hexagonal packing obtained by dropcasting from CH_2Cl_2.

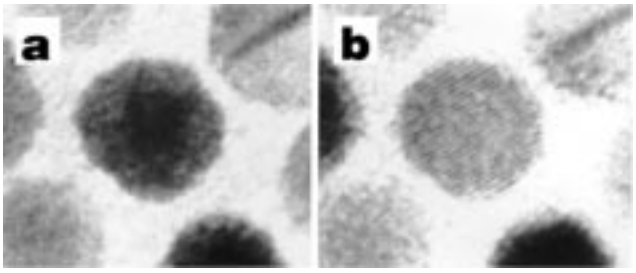

Figure 2. (a) Bright field and (b) tilted illumination TEM of a 5.9 nm ($N_A \sim 6350$ atoms[10]) Au-PDA nanocrystal showing characteristic [111] lattice fringes.

(1) For example: (a) Schön, G.; Simon, U. *Colloid Polym. Sci.* **1995**, *273*, 101−117. (b) Schön, G.; Simon, U. *Colloid Polym. Sci.* **1995**, *273*, 202−218. (c) Montemerlo, M. S.; Love, J. C.; Opiteck, G. J.; Goldhaber-Gordon, D.; Ellenbogen, J. C. "Technologies and Designs for Electronic Nanocomputers", MITRE Technical Report No. 96W0000044, MITRE Corporation: McLean, VA, 1996.

(2) Brown, L. O.; Hutchison, J. E. *J. Am. Chem. Soc.* **1997**, *119*, 12384−12385.

(3) Although thiolate-stabilized nanoparticles have received much attention in the past few years, passivation by amine-terminated molecules has remained largely unexplored. A significant problem has been that the preparative method popularized by Brust et al. leads to highly size-disperse nanoparticles when adapted to induce passivation by amines. (a) Brust, M.; Walker, M.; Bethell, D.; Schiffrin, D. J.; Whyman, R. *J. Chem. Soc., Chem. Commun.* **1994**, 801−802. (b) Leff, D. V.; Brandt, L.; Heath, J. R. *Langmuir* **1996**, *12*, 4723−4730.

(4) In our work we have utilized both aromatic (e.g., 4-fluoroaniline) and aliphatic (e.g., PDA) ligand types.

(5) Au-TPP was prepared according to the synthesis of $Au_{55}(PPh_3)_{12}Cl_6$: Schmid, G. *Inorg. Synth.* **1990**, *27*, 214−218.

(6) See Supporting Information for full procedure.

(7) The 7.2 nm nanocrystal listed in Table 1 is an example of this material.

(8) Brown, L. O.; Hutchison, J. E. Unpublished results.

(9) 369 particles measured. The measured size distribution may be slightly larger than the true value due to the inability to adequately distinguish overlapping small particles from single particles.

10.1021/ja983510q CCC: $18.00
Published on Web 01/15/1999

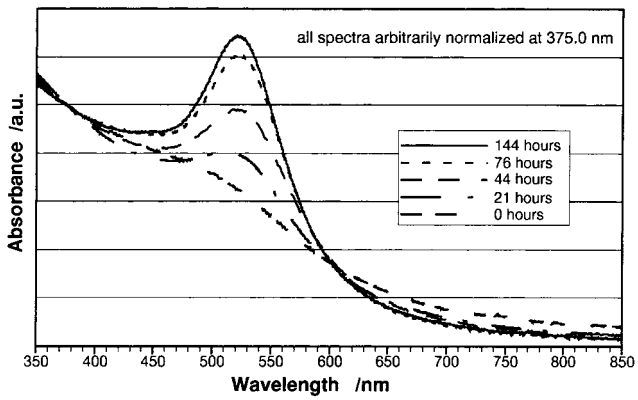

Figure 3. Progress of Au-TPP to Au-PDA followed by visible spectroscopy.

doublet is observed. The absence of chlorine and phosphorus ensures us that the ligand exchange process has gone to completion. However, as with previous reports of amine-stabilized nanoparticles, we are unable to observe a nitrogen signal,[3b] possibly due to X-ray damage or insensitivity of the technique to a small amount of nitrogen.

To determine that the amine ligands are bound to the gold core we obtained ^{1}H and ^{13}C NMR spectra. As expected, signals for nuclei close to the gold core are broadened into the baseline,[11] although the effect is not so great as observed for thiolate-stabilized nanoparticles. In the ^{13}C NMR, only the α- and β-resonances (at 42.36 and 34.01 ppm in free PDA) are unobservable.[12] Only a small degree of broadening affects the remaining resonances and shifts relative to the free amine are all less than 0.2 ppm. The ^{1}H NMR spectrum lacks the α-resonance at 2.6 ppm. An additional very broad signal is visible from ∼3.0 ppm to −0.5 ppm, in agreement with the observations of Heath et al.[3b]

A highly practical feature of our exchange method is that the final nanocrystal size is highly reproducible. For example, increasing the PDA concentration speeds the reaction rate but gives a similar size nanocrystal.[13] Using very small amounts of ligand gives a nanocrystal of similar size, but with a wider size distribution (e.g., 1.0:0.1 mass ratio of Au-TPP: PDA, Table 1).

A striking feature of the exchange reaction described herein is the controlled growth process leading to the final nanocrystal. This was not observed for the corresponding thiolate ligand exchanges.[2] A number of possible pathways can be considered. An obvious route involves stepwise aggregation in which two particles form a dimer. Two dimers can then produce a tetramer

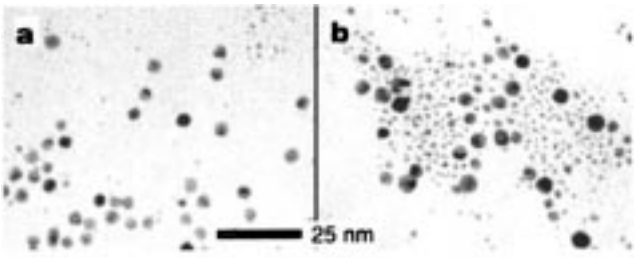

Figure 4. TEM images of Au-PDA corresponding to samples in Figure 3: (a) 21 h; (b) 44 h. Deposition by aerosol (CH_2Cl_2 solution). The relative populations of small and large particles vary greatly over the sample surface in each of the samples.[14]

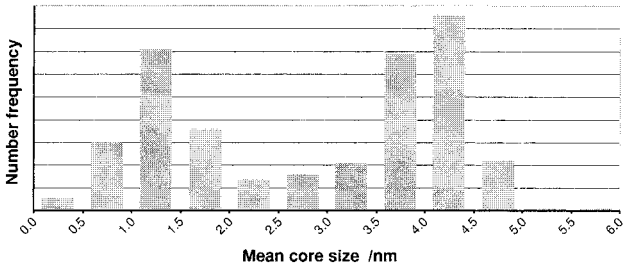

Figure 5. Size distribution of 373 nanoparticles in a TEM image of which Figure 4a is a small section.

and the process can continue until the final size is reached. To learn about the growth process, we examined an exchange reaction using a 1:2 mass ratio of Au-TPP to PDA. Visible spectra (Figure 3) and TEM images (Figure 4) were recorded at various times during the reaction. As expected, the intensity of the plasmon resonance band increases throughout the reaction, reflecting the increasing presence of larger particles. If the aggregation pathway described above was operational, a single size distribution should always be observed, yet the TEM data show a bimodal distribution of nanoparticles throughout the reaction course (e.g., Figure 5). While the larger particles show slow growth over time, the smaller particles remain a constant size. The completed reaction mixture shows none of the smaller particles. A pathway more consistent with the data would be one in which small nanoparticles slowly become "activated". These "activated" particles then grow by addition of the remaining unactivated particles until the supply of small nanoparticles is exhausted. The growth process is slow for the majority of the reaction time. A slow initiation/activation step is suggested by the visible spectra which show very little particle growth during the first few hours of the reaction.

In conclusion, we have presented a new approach to obtaining amine-stabilized nanocrystals of a well-defined size in solution under mild conditions. This work demonstrates the feasibility of controlling core size by variation of ligand. The product nanocrystals demonstrate highly ordered packing assisted by a very narrow size distribution, making them excellent candidates for the preparation of nanoscale devices.

Acknowledgment. We thank Eric Schabtach (UO Electron Microscope facility) for useful discussion and NSF for funding (NSF-DMR 9705343).

Supporting Information Available: Detailed procedure for producing Au-PDA from Au-TPP. ^{13}C NMR data for Au-PDA. Visible spectra comparing the progress of Au-TPP toward Au-PDA for differing reactant ratios (PDF). This material is available free of charge via the Internet at http://pubs.acs.org.

JA983510Q

(10) An approximate number of atoms, N_A, can be calculated for either (a) a particle radius in lattice spacings, n, using $N_A = (4\pi n^3)/3$, or (b) a particle diameter in distance, d, based on the packing density of bulk state gold: $d = (6N_A / 59\pi)^{1/3}$. From the second formula we would expect a 5.1 nm particle to be comprised of $Au_{\sim 4100}$. See also: Alvarez, M. M.; Khoury, J. T.; Schaaff, G.; Shafigulin, M. N.; Vezmar, I.; Whetten, R. L. *J. Phys. Chem. B* **1997**, *101*, 3706−3712.

(11) For example, see: (a) Terrill, R. H.; Postlethwaite, T. A.; Chen, C.-h.; Poon, C.-D.; Terzis, A.; Chen, A.; Hutchison, J. E.; Clark, M. R.; Wignall, G.; Londono, J. D.; Superfine, R.; Falvo, M.; Johnson, C. S., Jr.; Samulski, E. T.; Murray, R. W. *J. Am. Chem. Soc.* **1995**, *117*, 12537−12548. (b) Badia, A.; Singh, S.; Demers, L.; Cuccia, L.; Brown, G. R.; Lennox, R. B. *Chem. Eur. J.* **1996**, *2*, 359−369. (c) Badia, A.; Gao, W.; Singh, S.; Demers, L.; Cuccia, L.; Reven, L. *Langmuir* **1996**, *12*, 1262−1269.

(12) For ^{13}C NMR data, see Supporting Information.

(13) See for example the optical spectra given in the Supporting Information.

(14) For this reason, Figure 5 cannot be taken as an absolute size distribution. The mean diameters of the small and large particles do remain consistent across the sample surface.